25th ABCM International Congress of Mechanical Engineering
October 20-25, 2019, Uberlândia, MG, Brazil

COB-2019-366
DEPENDENCE OF ORIFICE PLATE PRESSURE DROP ON THE AREA RATIO FOR A GAS-LIQUID FLOW

Matheus Alexandre Pasquini
Eugênio Spanó Rosa
School of Mechanical Engineering – State University of Campinas, Mendeleyev Street 200, 13083-860, Campinas, SP, Brazil
m.alexandrepasquini@gmail.com
erosa@fem.unicamp.br

Abstract. *The dependence of the pressure drop on a gas-liquid mixture due the area contraction ratio is investigated for thin concentric orifice plate. The approach uses two-phase multipliers extracted from air-water experimental data with distinct pipe diameter, orifice's area contraction ratio operating in horizontal and vertical lines. The experimental data disclose for a fixed quality an increase on the two-phase multiplier as the orifice's contraction ratio increases. It is proposed an improvement on a two-phase multiplier model adding the influence of the orifice's area contraction ratio as a correction term into the slip ratio.*

Keywords: *orifice plate, pressure drop, two-phase multipliers.*

Nomenclature

A	pipe cross section area
D	pipe diameter
d	orifice diameter
J_k	superficial velocity of gas or liquid, $J_k = Q_k/A$ and $k = G$ or L.
M_k	mass flow rate of gas or liquid, $k = G$ or L.
Q_k	volumetric flow rate of gas or liquid, $k = G$ or L.
S	slip ratio, $S = u_G/u_L$
u_k	velocity of gas or líquid, $k = G$ or L.
s	orifice plate thickness
x	quality, defined as the ratio of the mass of gas to the mass of the mixture.
ΔP_{TP}	two-phase orifice's pressure drop.
ΔP_k	orifice's pressure drop for gas or liquid flow only, $k = G$ or L.
ρ_k	density of the gas or liquid, $k = G$ or L.
θ	Lin (1984) parameter based on the density ratio of the gas to the liquid phase.
ϕ_L^2	two-phase multiplier, see Eq.(1)
σ	orifice`s area contraction ratio; $\sigma = (d/D)^2$.

1. INTRODUCTION

The flow of a gas-liquid mixture in a pipeline in the presence of an area constraint is commonly found in processes involving power generation, chemical processes, on refrigeration applications and on the petroleum industry. The devices with area contraction ratio occur in passage through control valves, chokes, orifices plate and in a class of flow meters where the flow is proportional to the square root of the pressure difference. The choice to study the gas-liquid flow through a thin concentric orifice plate with sharp edges is because of the simple geometry and has well established theory for single-phase flow. The developments of single-phase applications were stretched out to gas-liquid flows with many valuable models and experimental data available.

The flow rate prediction in gas-liquid mixtures using concentric orifice plate was developed during the 1960 through 1980, approximately. The procedure employs two-phase multipliers combined with gas-liquid flow models. Usually the two-phase multipliers were used to estimate the orifice's pressure drop while the fluid models accounted for phenomena such as: incompressible or compressible flows, without or with slip and interfacial friction and with phase change inclusive. Many authors contributed to the development on this subject, we cite the works of Wallis (1969) and Chisholm

(1983) as representative of this period. Nonetheless, a short review significant to this paper, starts with Murdock (1962) who analyzed a large set of experimental data including air-water and also steam and liquid water for orifice plate. Murdock used the two-phase multiplier of the form of $(\Delta P_{TP}/\Delta P_G)^{1/2} = C_1$. $(\Delta P_L/\Delta P_G)^{1/2} + 1$, fitted the whole pressure data set and proposed a model to estimate the two-phase flow rate. Salcudean (1980) experimentally determined the two-phase multipliers defined in Eq. (1) for various forms of obstructions in an air-water flow. Lin (1982) experimental data comes from saturated mixture of liquid-vapor of R113. Lin (1982) proposes a correction on Murdock's constant C_1 by a 5th order polynomial, θ, as a function of the density ratio, ρ_L/ρ_G. Lin's final form of the two-phase multiplier is: $(\Delta P_{TP}/\Delta P_{JL})^{1/2} = \theta + x.\ [(\rho_L/\rho_G)^{1/2} - \theta]$ where x is vapor quality. The Lin's two-phase multipliers reported a bias of 10% against other experimental data sets.

More recently, Fossa and Guglielmini (2002) studied the influence of the orifice plate thickness in a horizontal experimental facility with air and water. Oliveira et al. (2009) performed experiments in a horizontal tube with an air water flow through an orifice plate coupled to a void fraction sensor. The objective was to determine parameters for optimization to the development of a new correlation to predict two-phase mass flow rate through orifice plates. Lastly, Zeghloul et al. (2017) compares the pressure drop predicted by different two-phase multipliers in a vertical upward flow through a set of orifice plates.

This work focuses on the orifice's pressure drop and its dependence on the orifice's contraction area ratio for flows with no phase change and no compressibility effects. The analyses are based on two-phase multipliers defined by Lockhart and Martinelli (1949) in Eq. (1):

$$\phi_L^2 = \Delta P_{TP} / \Delta P_L \ , \tag{1}$$

where ΔP_{TP} and ΔP_L represent the pressure drop at the orifice due: to the two-phase flow and to the liquid flow rate flowing alone. These ΔP values are determined experimentally. Also are used correlations for two-phase multipliers such as the homogeneous flow and three most frequently two-phase multipliers: Chisholm (1983), Simpson et al. (1983) and Morris (1985) shown on Tab. 1.

Table 1. Two-phase multipliers.

Reference	Correlations	Additional information
Homogenous flow	$\phi_L^2 = \frac{\rho_L}{\rho_G} x + (1 - x)$	none
Chisholm (1983)	$\phi_L^2 = 1 + \left(\frac{\rho_L}{\rho_G} - 1\right) \cdot [B \cdot x \cdot (1 - x) + x^2]$	B = 0.5 or 1.5 for thin and thick orifices respectively
Simpson et al. (1983)	$\phi_L^2 = [1 + x \cdot (S^{**} - 1)] \cdot \{1 + x \cdot [(S^{**})^5 - 1]\}$	$S^{**} = (\rho_L/\rho_G)^y$
Morris (1985)	$\phi_L^2 = \left[x \cdot \frac{\rho_L}{\rho_G} + S^* \cdot (1 - x)\right] \cdot \left[x + \left(\frac{1 - x}{S^*}\right) \cdot \left(1 + \frac{(S^* - 1)^2}{\sqrt{(\rho_L/\rho_G)} - 1}\right)\right]$	$S^* = \sqrt{1 + x \cdot \left(\frac{\rho_L}{\rho_G} - 1\right)}$

The slip ratio, S, is proportional to the phases' density ratio, (ρ_L/ρ_G). This is apparent comparing correlations S^{**} used by Simpson et al. (1983) and S^* employed by Morris (1985). In fact, S^* is the slip ratio correlation originally proposed by Chisholm (1983).

For gas-liquid mixtures, the effect of the operational pressure is transmitted to the ϕ_L^2 through the changes on the gas density. Figure 1 shows the ϕ_L^2 as a function of the quality, where Fig. 1a-b displays homogenous and Chisholm (1983) models while Fig. 1c-d represents Simpson et al. (1983) and Morris (1985) models.

The figure explores the dependency of ϕ_L^2 on the operational pressure changing from 100kPa through 1000kPa for an air-water mixture. For a fixed quality the value of ϕ_L^2 decreases as the pressure increases.

As the pressure increases from 100 kPa to 1000 kPa the models' proposed by Chisholm (1983), Simpson et al. (1983) and Morris (1985) tend to approach homogenous model exhibiting lower bias in regard the homogenous model.

A visual inspection on the ϕ_L^2 on Fig. 1 reveals similarity in shape and in the span. But a quantitative inspection discloses differences. Comparisons of ϕ_L^2 predicted by Chisholm (1983), Simpson et al. (1983) and Morris (1985) is drawn defining a relative difference based on Simpson ϕ_L^2 as given by Eq. (2)

$$\begin{aligned} \varepsilon\phi^2_{L,(C-S)} &= \left(\phi^2_{L,C} - \phi^2_{L,S}\right) \Big/ \phi^2_{L,S} \\ \varepsilon\phi^2_{L,(M-S)} &= \left(\phi^2_{L,M} - \phi^2_{L,S}\right) \Big/ \phi^2_{L,S} \\ \varepsilon\phi^2_{L,(C-M)} &= \left(\phi^2_{L,C} - \phi^2_{L,M}\right) \Big/ \phi^2_{L,S} \end{aligned} \ . \tag{2}$$

Where $\varepsilon{\phi_L}^2$ represents the relative difference among two-phase multiplier models indicated in the subscripts *C*, *S* and *M* representing Chisholm (1983), Simpson et al. (1983) and Morris (1983) respectively.

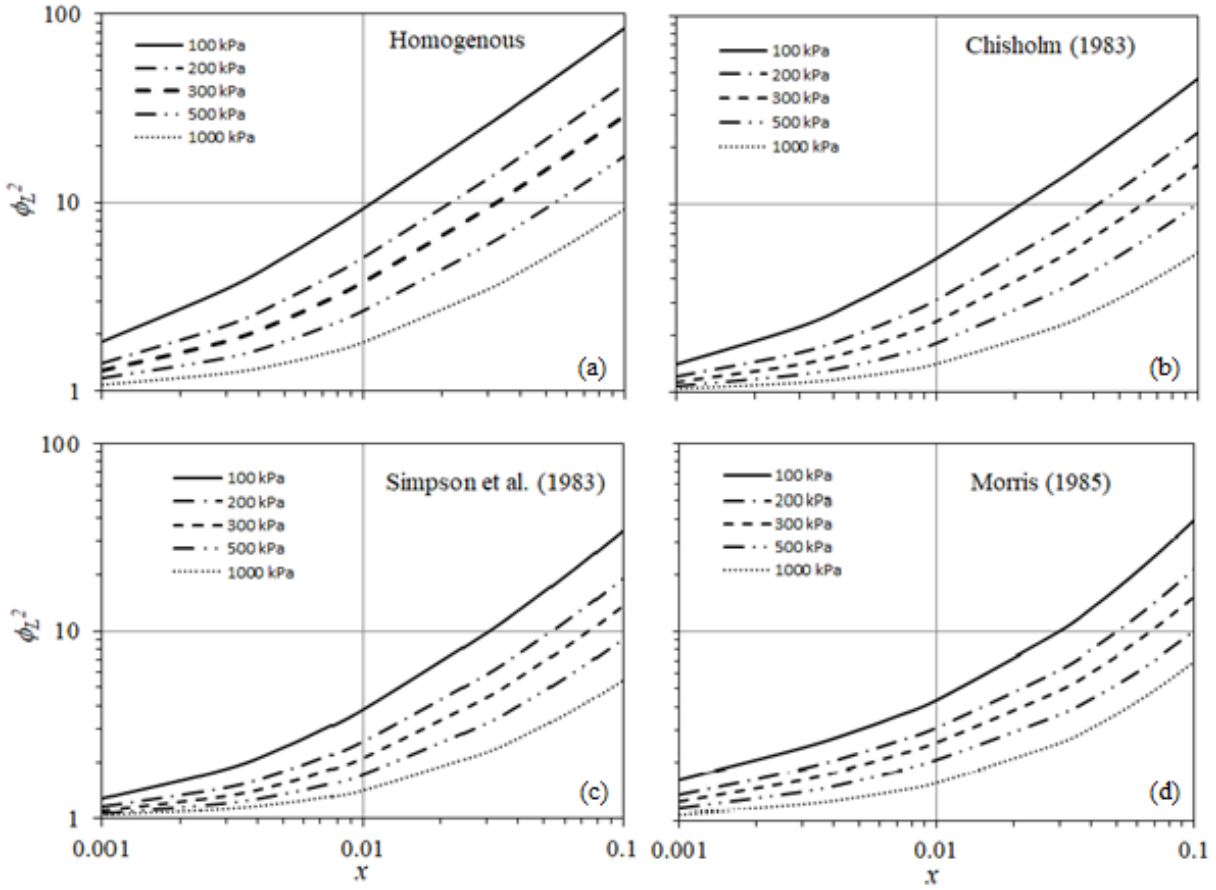

Figure 1. Two-phase multiplier as a function of the quality for air-water mixtures with pressure changing from 100 kPa to 1000 kPa. From left to right, the figures, correspond to the homogeneous, Chisholm, Simpson and Morris.

Figure 2 shows the relative differences among the ϕ_L^2 estimate given by Chisholm (1983), Simpson et al. (1983) and Morris (1985) at atmospheric pressure accordingly definition given on Eq. (2). The differences among Chisholm and Simpson span from +10% to +45%. The differences between Morris and Simpson span from +35% to +5%. The differences between Chisholm and Morris span from -20% up to +40%.

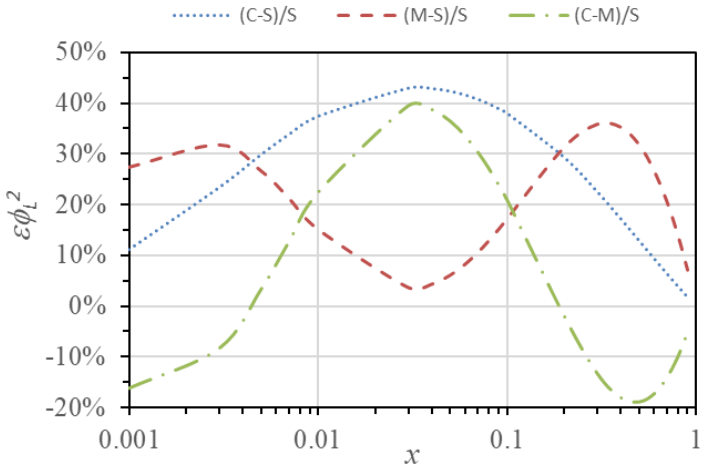

Figure 2. Relative differences among he ϕ_L^2 estimate given by Chisholm (1983), Simpson et al. (1983) and Morris (1985) accordingly definition given on Eq. (2).

The ϕ_L^2 correlations proposed by Chisholm (1983), Simpson et al. (1983) and Morris (1985) differ through the products and powers between *x* and (ρ_L/ρ_G). These factors explain the differences among these ϕ_L^2 seen on Fig. 2.

Despite Simpson's ϕ_L^2 also has a similar structure with products and powers of *x*, (ρ_L/ρ_G) it has an important feature not present on the others ϕ_L^2. Simpson's allows one degree of freedom on the slip ratio, specifically the parameter *y* on the density ratio: $(\rho L/\rho G)^y$.

The parameter *y* is free to change from 0 up to ½, corresponding for no-slip to the maximum slip independently of *x*. For general applications, Simpson et al. (1983) recommend *y* = 1/6.

Figure 3 explore the changes on the slip ratio varying the parameter *y*: $S = (\rho_L/\rho_G)^y$, for a air-water mixture at 300 kPa. For a fixed *x*, ϕ_L^2 increases as *y* increases. Complementary, as *y* move toward zero slip ration approaches unit indicating that the gas-liquid mixture pressure drop is equal to the phases' pressure drop.

As the mixture approaches the orifice from upstream the phases' velocities increase due the area contraction. The interplay among the phase velocities, densities and the void fraction is complex. Nonetheless Simpson et al. (1983) quotes: "It might be expected that *y* will lie the lower values because of the flow with area restriction suppresses the phase's separation and hence the slip". Maidana and Rosa (2018) filmed the slug flow going through orifice plates and is possible to see that the separated gas-liquid along the elongated bubble is broken near the orifice in a dispersed gas-liquid reducing de slip between the gas and liquid.

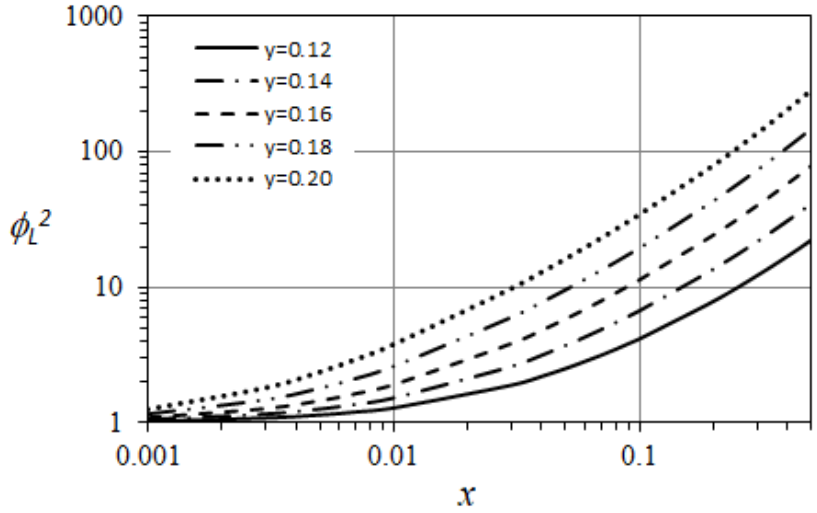

Figure 3. Simpson's ϕ_L^2 sensitivity on parameter y for air-water mixture at 300 kPa.

The theory of orifice plate for single phase shows dependence of the flow rate to the area contraction. This paper investigates the dependence of ϕ_L^2 on the area contraction ratio. A search of a better adjust on parameter *y* to give a minimum RMS error between the experimental data and the Simpson's ϕ_L^2. The optimum *y* employs a non-linear least square routine to minimizes the RMS error. Further, it is determined a correlation between *y* and σ to increase the accuracy of Simpson ϕ_L^2.

Some hints about the dependency of ϕ_L^2 on σ is found in Alimonti et al. (2010). During the development of a model for a valve with multiple orifices with variable area propose the use of coefficient, K_v, as a function of the percentage of the valve aperture. Also, Maidana and Rosa (2018) analyzing the pulsating effect induced by the passage of slug flow through orifices with different area contraction found a linear relationship between the two-phase multiplier and the area contraction ratio for a fixed gas and liquid flow rate.

In order to encompass area contraction ratio spanning from 0.072 to 0.730 an experimental campaign to add to the available data on the literature, experimental data for data for σ = 0.072 and 0.123 not available in the literature, see Appendix 1 at the end of the paper.

The paper structure describes the experimental apparatus and procedure on Section 2. The data base is on Section 3. The comparison against the two-phase multipliers, the dependency of the orifice´s on the area contraction ratio is on Section 4. Finally, Section 5 shows the conclusions.

2. EXPERIMENTAL APPARATUS AND EXPERIMENTAL PROCEDURE

The schematic diagram of the experimental apparatus is in Fig. 4; the colored lines blue, green and red represent, respectively, the air flow, water flow and the air-water mixture on the test section. The test fluids are compressed air which is considered ideal with a constant R = 287 J / kg.K, and water which is of a density of 998 kg / m^3 and a viscosity of 0.001 Pa.s. The water and air lines are supplied respectively by a centrifugal pump and by three compressors installed in a series of maximum flow of 0.085Nm^3/ s to 1206.6 KPa.

The mass flow rates of the fluids are determined, the air flow uses a sonic nozzle, manufactured in house and the water flow employs a Coriolis mass flow meter. The air and water flow are controlled by two globe valves. The steady flow of air is assured, despite the pressure fluctuations of the test section, due the chocked conditions of the nozzle. The disturbances on the water flow is minimized setting the globe valve almost closed to increase the pressure upstream the valve thus minimizing the pressure disturbances downstream.

The flows of air and water are mixed at the beginning of the test section. The test section has a transparent acrylic horizontal tubing with an internal diameter of 26 mm and 26.24 m (1009 D) length. The absolute pressure is measured along the test section and also the differential pressure at the orifice plate located at 634D from the injector nozzle.

The two-phase flow is discharged into a $3m^3$ tank open to the atmosphere. The tank is used as a flow separator; the air vents to the atmosphere and the water is pumped back into the initial tank. The atmospheric conditions are, approximately, of 94 KPa and 25°C.

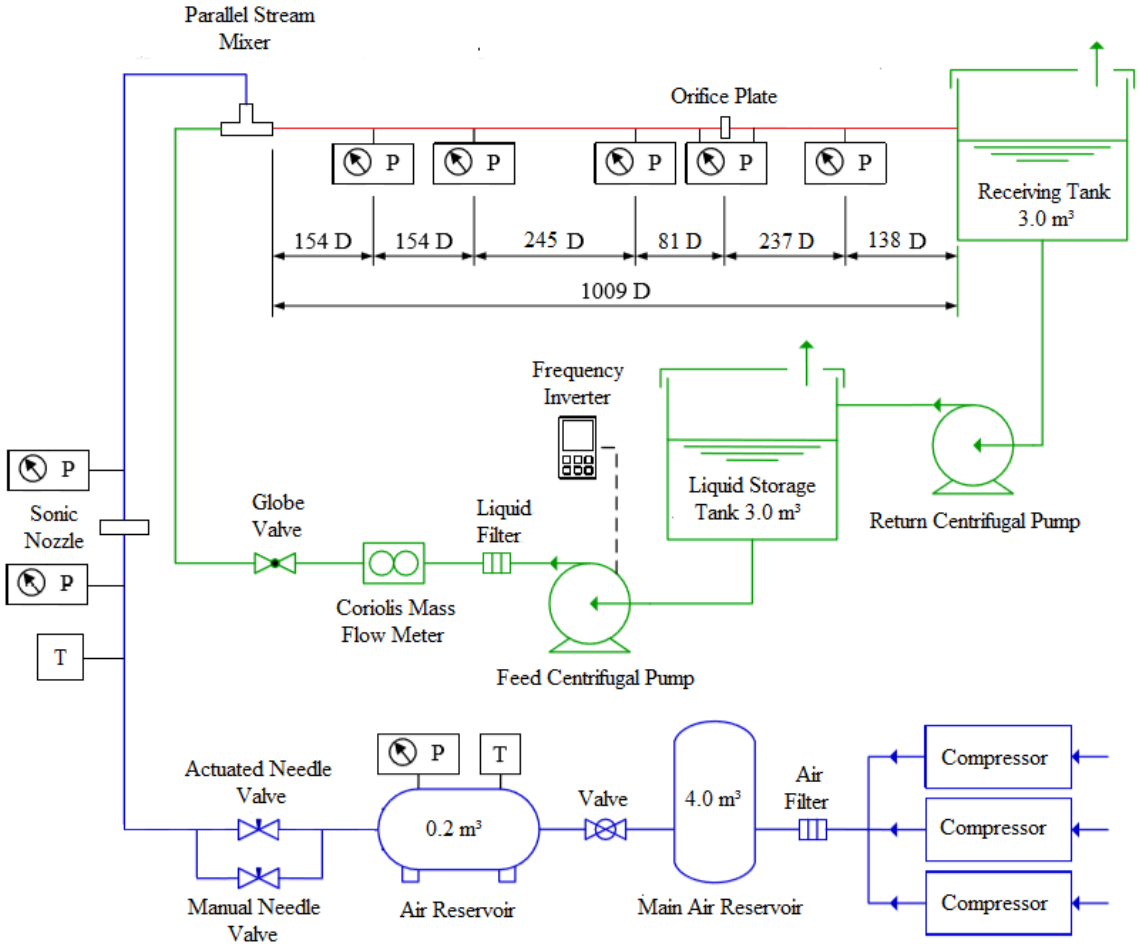

Figure 4. Experimental apparatus schematic. (Adapted from Maidana and Rosa, 2018).

Two orifice-plates, with internal diameters of 0.007m and 0.009m were used during the experimental campaign. The orifices have an area contraction ratios σ, of 0.072 and 0.0123 respectively. The ratio between the plate thickness, s, and the orifices' internal diameter, d, are respectively 0.429 and 0.330. According to the criterion of Chisholm (1983) both orifice plates are considered thin, i.e $s/d \leq 0.5$. The orifice's mean pressure drop is measured by flange taps from a sample of ten runs lasting two minutes each run and sampled at 3000 points per second. The volumetric and the mass flow rate are determined. The quality is determined accordingly Eq. (3).

$$x = M_G / \left(M_G + M_L \right), \tag{3}$$

where M represents the mass flow rate the subscripts G and L represents the liquid and gas phases respectively.

The test section operates with slug flow pattern only. Each experimental run lasts 120 seconds which corresponds to 100 slugs, approximately. The absolute pressure along the test section and the pressure difference at the orifice are

recorded at a 3000 samples per second. The air and the water flows are recorded at 2 samples per second. To get the average pressures the procedure is repeated 10 times which amounts nearly 1000 slug units to get the average pressure.

3. THE DATA BASES

The analyses are based on eight data bases shown on Tab. 2. All orifice plates used along the analyses are thin, accordingly to Chisholm (1983) criterion. The tests #1 and #2 refer to the experimental campaign described in Section 2, with σ of 0.072 and of 0.123, respectively. Text #3 refer to Oliveira et al. (2009) experimental data with σ of 0.25 and pressure ranged of 200 to 300 kPa. Simpson et al. (1983) experimental data with $\sigma =$ 0.25 and $\sigma = 0.563$ in 127mm inner diameter horizontal pipe is represented by texts #4 and # 7. Next the data from Zeghloul et al. (2017) in a vertical line, 6m long, the orifice plate is located at 4110 mm downstream of air water mixer with σ of 0.533 represented by texts #5. Lastly, tests #6 and #8 bring the experimental data from Fossa and Guglielmini. (2002) for horizontal flow with σ of 0.54 and 0.73 respectively.

Table 2. Data bases.

Data base	Authors	s/d	Inlet diameter [mm]	σ	Position	Number of points
#1	Pasquini and Rosa	0.429	26	0.072	Horizontal	12
#2	Pasquini and Rosa	0.330	26	0.123	Horizontal	18
#3	Oliveira et al. (2009)	0.143	21	0.250	Horizontal	24
#4	Simpson et al. (1983)	N.A.	127	0.250	Horizontal	35
#5	Zeghloul et al. (2017)	0.2	34	0.533	Vertical	70
#6	Fossa and Guglielmini (2002)	0.027 to 0.2	40	0.540	Horizontal	10
#7	Simpson et al. (1983)	N.A.	127	0.563	Horizontal	52
#8	Fossa and Guglielmini (2002)	0.027 to 0.2	40	0.730	Horizontal	12

3.1 Data comparison of two-phase multipliers against correlations

Table 3, disclose the RMS error of each experimental data against the two-phase multipliers represented in Tab. 1 where the least RMS error values are represented by bold characters. Tests #1, #2 and #3 have the least RMS error using Simpson with 1/6 *y* parameter. Tests #4 and #5 have the least RMS error using, respectively, Simpson with 1/6 and Morris. Test #6 and #7 has the least RMS using Chisholm and Morris model. Lastly test #8 has the least RMS error using homogenous model. Table 3 reveals the homogenous model gave the worst forecast, despite of test #8. This information reveals the slip plays a significant role in define two-phase pressure drop through the area contraction ratio.

Table 3. RMS deviation between the experimental data and correlations

Correlations / Tests	#1	#2	#3	#4	#5	#6	#7	#8
Homogeneous	1.4122	1.4020	1.0957	10.6408	2.8553	1.4287	17.8847	**0.4326**
Chisholm (1983)	0.5540	0.4808	0.3013	12.7537	0.9276	**0.2136**	6.0147	0.5921
Simpson et al. (1983)	**0.2681**	**0.1665**	**0.1465**	**6.8894**	0.7064	0.6943	**3.1439**	0.8568
Morris (1985)	0.7165	0.6407	0.4376	9.1437	**0.5776**	0.2584	3.6189	0.4983

Figure 5 displays the experimental data against the prediction given by the two-phase multipliers on Tab. 1. The y-axis corresponds to the two-phase multiplier while the x-axis is the quality. The scattered open circles represent the experimental data while the continuous lines are the two-phase multiplier $\phi_L{}^2$ model predictions.

Figure 5 displays the experimental data sets against the used $\phi_L{}^2$ models. A visual inspection on Fig. 5 strengthen best fits of $\phi_L{}^2$ found on Tab. 3. Tests #1 and #2, are over estimated, but the closest forecast is the Simpson with *y*=1/6. Tests #3 and #4 are better represented by Simpson with $y = 1/6$. Test #5 has the experimental data crossing the lines predicted by Simpson, Morris and Chisholm due large data scattering. Test #6 and #7, have the data crossing the lines of Chisholm and Morris, in particular, test #7 exhibits large data scattering. Lastly test #8 has the experimental data crossing the two-phase multipliers from Simpson, Morris, Chisholm and homogenous model despite the low data scattering.

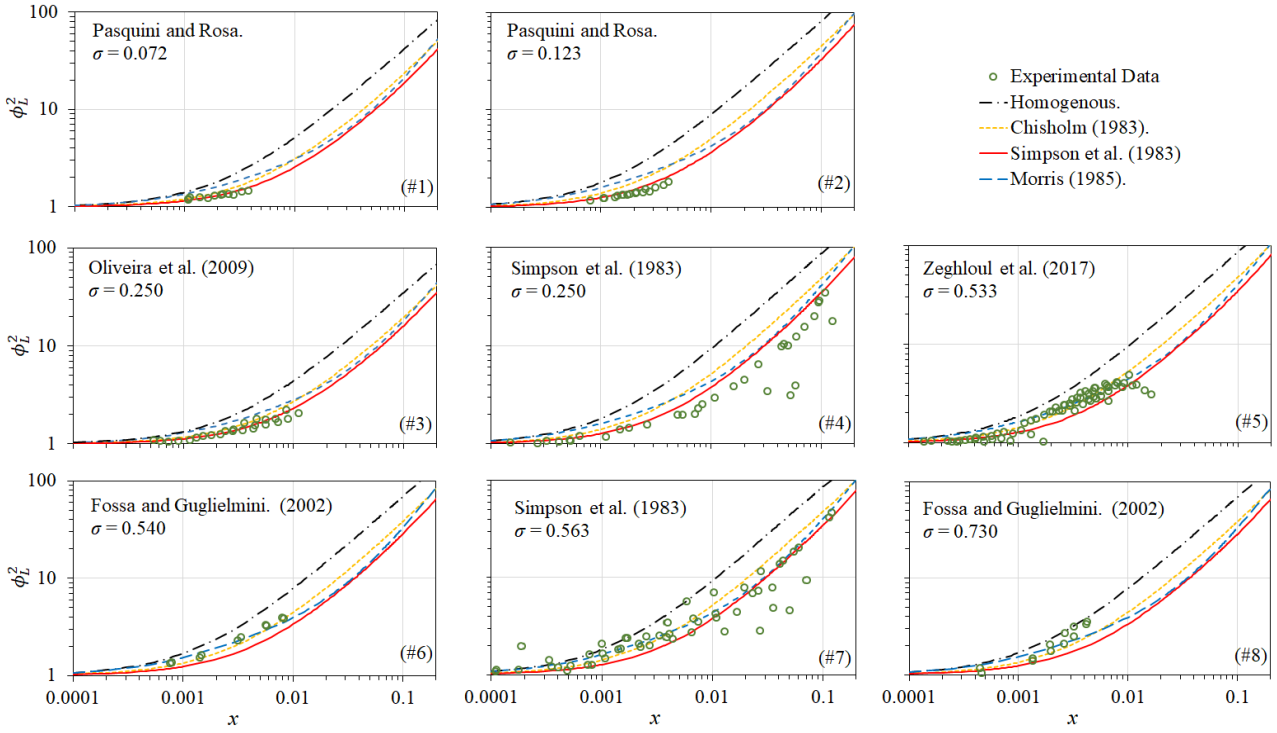

Figure 5. Comparison of ϕ_L^2 experimental versus quality against ϕ_L^2 model given in Tab. 1.

4. THE VARIABLE Y PARAMETER

Using the fact that parameter *y* on Simpson et al. (1983) correlation span from 0 to 1/2, we decided to determine the best slip ratio which minimize the RMS error. The search of minimum RMS ends up finding the best parameter *y* which minimizes RMS for each data basis.

Table 4 displays the best parameter *y* for each data basis, the RMS error and also the area contraction ratio. There is a reduction on the RMS error for the data bases if compared against the RMS error displayed on Tab.3.

Table 4. Best *y* parameter for the experimental data base.

Tests	#1	#2	#3	#4	#5	#6	#7	#8
Best parameter *y*	0.1486	0.1574	0.1618	0.1537	0.1692	0.1814	0.1646	0.1929
Orifice contraction ratio, σ	0.072	0.123	0.250	0.250	0.533	0.540	0.563	0.730
RMS deviation	0.0647	0.0337	0.1205	3.7825	0.6945	0.1346	3.0588	0.2555

Table 4 also discloses that the best *y* parameter is proportional to the area contraction ratio. The tests #5 and #7 were not used to find a dependence of *y* on the σ due the large data scattering . Figure 6 shows a liner relationship between *y* and σ using tests #1, #2, #3, #4, #6 and #8.

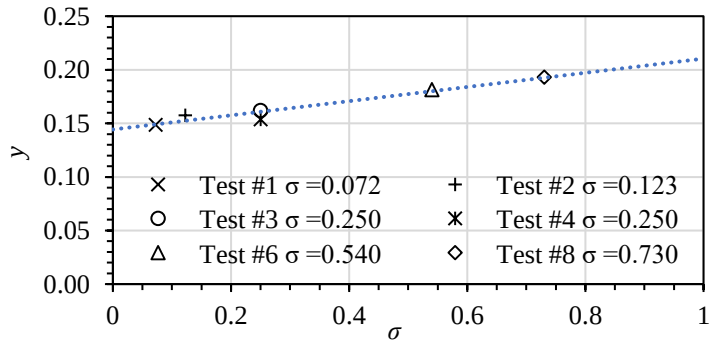

Figure 6. Linear Fit to the relation of area contraction ratio σ and parameter *y*

The dependency of parameter *y* to σ is in Eq. (4):

$$y = 0.0661 \cdot \sigma + 0.1443, \tag{4}$$

with a R square parameter of 95% and valid for the $0{,}07 \leq \sigma \leq 0{,}73$.

The RMS error between each experimental base and the Simpson ϕ_L^2 of using *y* given by Eq. (4) is shown in Tab.5.

Table 5. The best parameter *y* estimate from Eq. (4) and the RMS error.

Tests	#1	#2	#3	#4	#5	#6	#7	#8
Best parameter y	0.1491	0.1524	0.1608	0.1608	0.1793	0.1800	0.1815	0.1926
RMS	0.0649	0.0769	0.1215	4.7279	0.9514	0.1565	8.4636	0.2561

A comparison of RMS errors using Tab. 5 against Tab. 3 is on Tab. 6 below:

Table 6. Comparison against minimum RMS in Table 3 and Table 5 RMS.

Correlations	#1	#2	#3	#4	#5	#6	#7	#8
Table 3 min. RMS	0.2681	0.1665	0.1465	6.8894	0.5776	0.2136	3.1439	0.4326
Table 5 RMS	0.0649	0.0769	0.1215	4.7279	0.9514	0.1565	8.4636	0.2561
Difference	0.2032	0.0896	0.0250	2.1615	-0.3738	0.0571	-5.3197	0.1765

Table 6 discloses the RMS error difference between minimum RMS error from Tab. 3 and RMS error of Simpson et al. (1983) model, with *y* parameter predict by Eq. (4). The tests #1, #2, #3, #4, #6 and #8 presents, respectively a reduction on the RMS values of 0.2032, 0.0897, 0.0250, 2.1615, 0.0357 and 0.1765. Test #5 and # 7 have the RMS error increased by 0.3738 and 5.3197. The difference expressed on Table 6 can also be as the relative error expressed in terms of Tab. 3 RMS error. Evaluating the relative RMS error, one finds a reduction of the RMS for tests #1, #2, #3, #4, #6 and #8 of 76%, 54%, 17%, 31%, 27% and 41% respectively. Test #5 and #7 the RMS error increase of 65% and 169% respectively. Inspection on Fig. 5 disclose large data scattering on test #5 and #7 exhibiting several values of ϕ_L^2 for a single value of *x*!

5. CONCLUSION

This work proposes a dependency on the slip ratio based on the area contraction ratio for a thin concentric orifice plate. The slip ratio dependence is expressed through the *y* parameter as a linear function of area contraction ratio, σ. The correction applies low quality due the limitations of the available data basis and no-compressible effects. The introduction of the dependence of *y* as a function of σ on the Simpson two-phase multiplier reduced the RMS error as compared the estimates of ϕ_L^2 against the experimental data.

6. ACKNOWLEDGEMENTS

This study was financed in part by the Coordenação de Aperfeiçoamento de Pessoal de Nível Superior - Brasil (CAPES) - Finance Code 001.

7. REFERENCES

Alimonti, C., Falcone, G., & Bello, O. (2010). Two-phase flow characteristics in multiple orifice valves. *Experimental Thermal and Fluid Science*, *34*(8), 1324-1333.

Chisholm, D. (1983). *Two-phase flow in pipelines and heat exchangers*. G. Godwin in association with Institution of Chemical Engineers.

Fossa, M., & Guglielmini, G. (2002). Pressure drop and void fraction profiles during horizontal flow through thin and thick orifices. *Experimental Thermal and Fluid Science*, *26*(5), 513-523.

Lin, Z. H. (1982). Two-phase flow measurements with sharp-edged orifices. *International Journal of Multiphase Flow*, *8*(6), 683-693.

Lockhart, R. W., & Martinelli, R. C. (1949). Proposed correlation of data for isothermal two-phase, two-component flow in pipes. *Chem. Eng. Prog*, *45*(1), 39-48.

Maidana, N.C., & Rosa, E. S. (2018). Flow disturbances induced by an orifice plate in a horizontal air-water flow in the slug regime. *Experimental Thermal and Fluid Science*, *94*, 59-76.

Morris, S. D. (1985, June). Two phase pressure drop across valves and orifice plates. In *Proceedings of the European Two Phase Flow Group Meeting, Marchwood Engineering Laboratories, Southampton, UK*.

Murdock, J. W. (1962). Two-phase flow measurement with orifices. *Journal of basic engineering*, *84*(4), 419-432.

Oliveira, J. L. G., Passos, J. C., Verschaeren, R., & Van Der Geld, C. (2009). Mass flow rate measurements in gas–liquid flows by means of a venturi or orifice plate coupled to a void fraction sensor. *Experimental Thermal and Fluid Science*, *33*(2), 253-260.

Salcudean, M., Groeneveld, D. C., & Leung, L. (1983). Effect of flow-obstruction geometry on pressure drops in horizontal air-water flow. *International journal of multiphase flow*, *9*(1), 73-85.

Simpson, H. C., Rooney, D. H., & Grattan, E. (1983). Two phase flow through gate valves and orifice plates. In *International conference on the physical modelling of multi-phase flow* (pp. 25-40).

Zeghloul, A., Azzi, A., Saidj, F., Messilem, A., & Azzopardi, B. J. (2017). Pressure drop through orifices for single-and two-phase vertically upward flow—implication for metering. *Journal of Fluids Engineering*, *139*(3), 031302.

Wallis, G.B. One dimensional two-phase flow. McGraw Hill, 1969.

6. RESPONSIBILITY NOTICE

The authors are the only responsible for the printed material included in this paper.

Appendix 1

Experimental data values obtained by authors. The tests are carried at near atmosphere pressure with the superficial velocities of air and water, J_G and J_L ranged from 0.3 m/s to 0.8 m/s and from 0.2 to 0.4 m/s respectively. The pressure transducers have uncertainty of 4%. J_G and J_L values have uncertainty of 0.3% and 1.4% respectively.

σ	J_L [m/s]	J_G [m/s]	mg [kg/s]	mL [kg/s]	ΔPtp kPa	ΔPL kPa	ρG [kg/m³]	x
0.072	0.199	0.262	0.00017	0.10533	9.9	8.0	1.23	0.00162
0.072	0.299	0.238	0.00017	0.15843	20.7	17.0	1.35	0.00108
0.072	0.199	0.347	0.00023	0.10536	10.6	8.0	1.24	0.00216
0.072	0.298	0.236	0.00017	0.15840	21.3	17.0	1.36	0.00111
0.072	0.396	0.281	0.00023	0.20973	35.2	29.6	1.51	0.00107
0.072	0.196	0.441	0.00029	0.10380	10.7	8.0	1.23	0.00277
0.072	0.298	0.406	0.00029	0.15787	22.2	17.0	1.36	0.00186
0.072	0.398	0.357	0.00029	0.21095	37.3	29.6	1.54	0.00138
0.072	0.199	0.527	0.00035	0.10547	11.6	8.0	1.26	0.00332
0.072	0.300	0.478	0.00035	0.15902	23.2	17.0	1.39	0.00222
0.072	0.198	0.594	0.00040	0.10514	11.8	8.0	1.26	0.00377
0.072	0.298	0.537	0.00040	0.15780	23.2	17.0	1.40	0.00253
0.123	0.199	0.268	0.00017	0.10567	4.1	3.0	1.16	0.00157
0.123	0.301	0.263	0.00017	0.15929	8.3	6.7	1.21	0.00106
0.123	0.400	0.260	0.00017	0.21172	13.9	11.6	1.22	0.00080
0.123	0.199	0.362	0.00022	0.10531	4.3	3.0	1.16	0.00211
0.123	0.300	0.348	0.00023	0.15915	8.8	6.7	1.22	0.00142
0.123	0.400	0.328	0.00023	0.21196	14.6	11.6	1.30	0.00107
0.123	0.201	0.442	0.00027	0.10636	4.6	3.0	1.16	0.00255
0.123	0.300	0.424	0.00028	0.15917	9.0	6.7	1.23	0.00173
0.123	0.399	0.404	0.00028	0.21145	14.9	11.6	1.31	0.00133
0.123	0.198	0.526	0.00033	0.10496	4.8	3.0	1.18	0.00314
0.123	0.300	0.521	0.00034	0.15896	9.5	6.7	1.24	0.00211
0.123	0.400	0.481	0.00034	0.21173	15.6	11.6	1.32	0.00160
0.123	0.198	0.613	0.00039	0.10487	5.2	3.0	1.19	0.00367
0.123	0.300	0.582	0.00038	0.15879	9.6	6.7	1.25	0.00242
0.123	0.400	0.546	0.00039	0.21192	15.9	11.6	1.33	0.00182
0.123	0.201	0.697	0.00044	0.10650	5.5	3.0	1.20	0.00414
0.123	0.300	0.660	0.00044	0.15875	9.8	6.7	1.25	0.00275
0.123	0.400	0.618	0.00044	0.21212	16.3	11.6	1.34	0.00207